

Multi-Axis Planning System (MAPS) for Hybrid Laser Metal Deposition Processes

Frank Liou, Jianzhong Ruan, Todd E. Sparks

Department of Mechanical and Aerospace Engineering
Missouri University of Science and Technology,
Rolla, MO

Reviewed, accepted September 23, 2010

Abstract

This paper summarizes the research and development of a Multi-Axis Planning System (MAPS) for hybrid laser metal deposition processes. The project goal is to enable the current direct metal deposition systems to fully control and utilize multi-axis capability to make complex parts. MAPS allows fully automated process planning for multi-axis layered manufacturing to control direct metal deposition machines for automated fabrication. Such a capability will lead to dramatic reductions in lead time and manufacturing costs for high-value, low-volume components with high performance material. The overall approach, slicing algorithm, machine simulation for planning validation, and the planning results will be presented.

I. Introduction

Layered Manufacturing (LM) technology has provided an efficient approach to build parts directly from a CAD model [e.g., 1-5] since its appearance in mid 80s in last century. Most of the current RP systems are built on a 2.5-D platform. Among them, the laser-based deposition process is a potential technique that can produce fully functional parts directly from a CAD system and eliminate the need for an intermediate step. However, such a process is currently limited by the need of supporting structures – a technology commonly used in all the current RP systems. Support structures are not desirable for high strength and high temperature materials such as metals and ceramics since these support structures are very difficult to move. As a result, the current laser deposition process, such as LENS (Laser Engineering Net Shaping [6]) from Optomec Inc., can only build fully dense metal with relatively simple geometry [7,8]. Therefore, building parts with complicated shapes becomes a hurdle for the process due to limited motion capability.

In order to expand the applications of metal deposition processes, multi-axis capability is greatly needed. A multi-axis rapid manufacturing system can be hardware-wise configured by adding extra degrees of mobility to a deposition system or by mounting a laser deposition device on a multi-axis robot. The configuration could also be a hybrid system in which a metal deposition system is mounted on a multi-axis CNC machine. With the addition of extra rotations, the support structures may not be necessary for the deposition process in order to build a complicated shape. Figure 1 illustrates the process to build an overhang structure on a 2.5D and multi-axis deposition system. Due to the nature of the deposition process, it is driven by a so-called “slicing” procedure, which uses a set of parallel planes to cut the object to obtain a series of slicing layers. So far, the slicing software on the market is only able to handle 2.5D slicing in

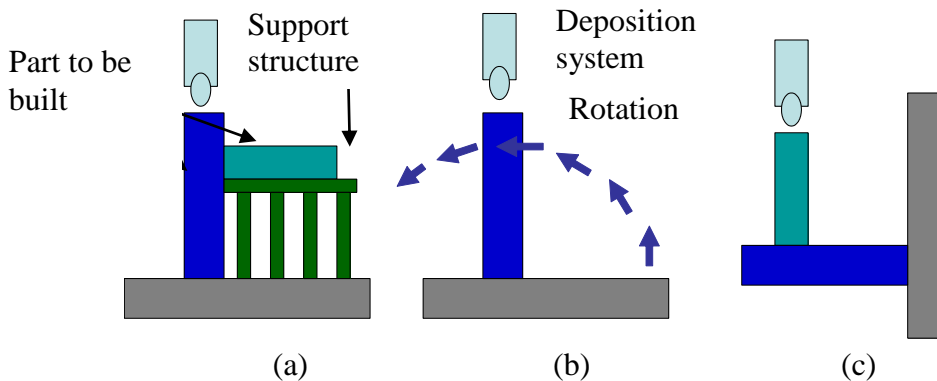


Figure 1: (a) build part with support structure; (b) with multi-axis capability, after building the column, the table can be rotated; (c) After rotation, continue to build the component from which the building/slicing direction is kept unchanged (usually Z+ direction) and it lacks the capability of changing directions to fully explore the capability of multiple degrees of freedom.

A solution to this problem is to change the slicing/building direction as needed, which could eliminate or decrease the usage of a support structure to build overhangs or complicated shapes. This paper introduces a Multi-Axis Planning System designed to drive a multi-axis hybrid laser metal deposition process. The overall approach, slicing algorithm and machine simulation will be discussed respectively. The paper is organized as follows: In section 2, slicing methods and overall approach are summarized; then the research problem for this paper is defined and the slicing algorithm will be discussed section 3 as well as the 2D path planning. The machine simulation will be presented in section 4. Some examples are shown in section 5. The paper is concluded in section 6.

II. Overall Approach

1. Previous Work

In LM processes, slicing is the process that is represented as a set of layers formed by "slicing" a CAD model with the set of horizontal planes [9]. The distance between planes is called "layer thickness". Differences in quality can be achieved by controlling the layer thickness. Research on 2.5-D slicing procedures and deposition toolpath for layered manufacturing processes has been widely conducted. Cusp height is introduced [10] to control the tolerance. Since then, various efficient and reliable processes for 2.5-D slicing procedures have been studied based on controlling cusp height and meeting the critical surfaces [11-14]. Some researchers presented a slicing method using volume difference between adjacent slicing layers [15, 16]. Rather than computing the cusp height, this method determines layer thickness by comparing the area difference between two neighboring layers after conducting Boolean operations. All these methods do not adopt multi-axis into slicing algorithm; thus, they lack the ability to handle a more complicated multi-axis layered manufacturing process. To some extent, these methods help to improve the efficiency and quality for the deposition system; however, not all of these methods adopt multi-axis into the slicing algorithm; thus, they lack the ability to handle a more complicated multi-axis layered manufacturing process.

Recently, some research has been focused on multi-axis slicing to drive the multi-axis deposition system in order to deliver a more efficient manufacturing system. The project method is reported to be used to find the new building direction for overhang structure [17]. In this work, the part is decomposed according to the projected information. The building direction is determined from a building map constructed for a decomposed component. However, in some cases, the building direction does not match the surface normal, which leads to a greater staircase effect. Furthermore, a collision may occur which is difficult to avoid. Figure 2 shows an example to illustrate this situation.

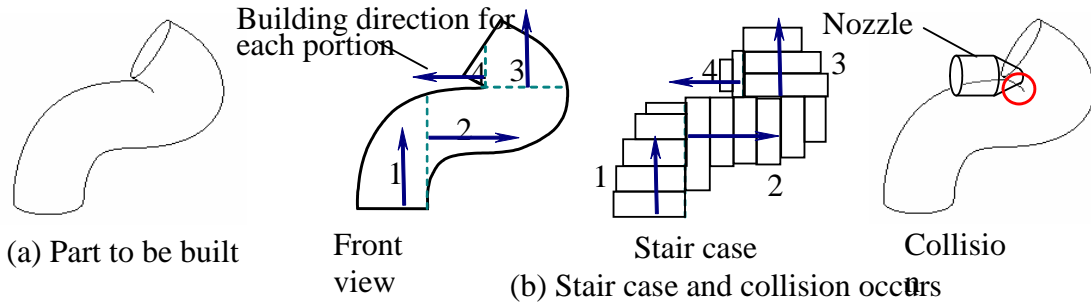


Figure 2: A case study to demonstrate limitation of projection-based method

A thin/transition wall concept has been presented to build overhang structures on the platform of the multi-axis deposition process. In this method, the building/slicing direction of one slice is determined by the previous layer. To build an overhang structure, the machine is turned 90° to start depositing a transition, named thin wall. After the wall is finished, the part is flipped back to its original direction to continue the deposition process. In this method, a so called 3-D slicing to generate non-uniform thickness layers is used to slice the curve (freeform) surface. However, transition/thin wall method does not consider possible collision and the planning result cannot be realized in the deposition system [18,19]. The slicing methods are summarized in Table 1.

Table 1. Slicing methods summary

Slicing method	Degree	Control Parameter	Limitation
Cusp height/volumetric difference[10,16]	2.5D	Cusp height/volumetric difference	Only suitable for regular 2.5D system
Projection [17]	Multi-axis	Cusp height	Collision and geometry error
Transition Wall [18]	Multi-axis	Cusp height	Hard to implement on physical machine

2. Overall approach

The difficulty of developing a capable multi-axis slicing algorithm lies in automatic slicing direction change. In a multi-axis slicing process, direction change is highly dependent on the geometry shape. Therefore, shape comprehension plays a crucial role in accurately predict the

slicing direction change. Medial axis, also referred to as skeleton, has been introduced to study biological shape for a long time [20]. Medial axis represents 3-D shapes with a series of curves/points, like the skeleton of a human body. This concept has been widely used in pattern recognition, shape analysis, and mesh generation [21]. Medial axis simplifies complex shapes and makes shape comprehension relatively easy. Thus, MAPS will use this tool to guide multi-axis slicing process. However, a slicing direction obtained from the medial axis is an initial guess. A more accurate slicing direction should be found based on the error check. MAPS will identify a final slicing direction for a layer so that the layer thickness is not beyond the maximum layer thickness and the errors (such as cusp height) are within the defined limit.

Multi-axis LM machines may have different machine configurations. Some motion systems are CNC type, in which each axis controls one DOF. Others may use robot type motion system. In order to validate result of MAPS for different kinds of hardware configurations, a generic machine description format will be researched and designed to allow MAPS to simulate the process planning for each machine configuration seamlessly. Figure 3 shows the overall approach for MAPS.

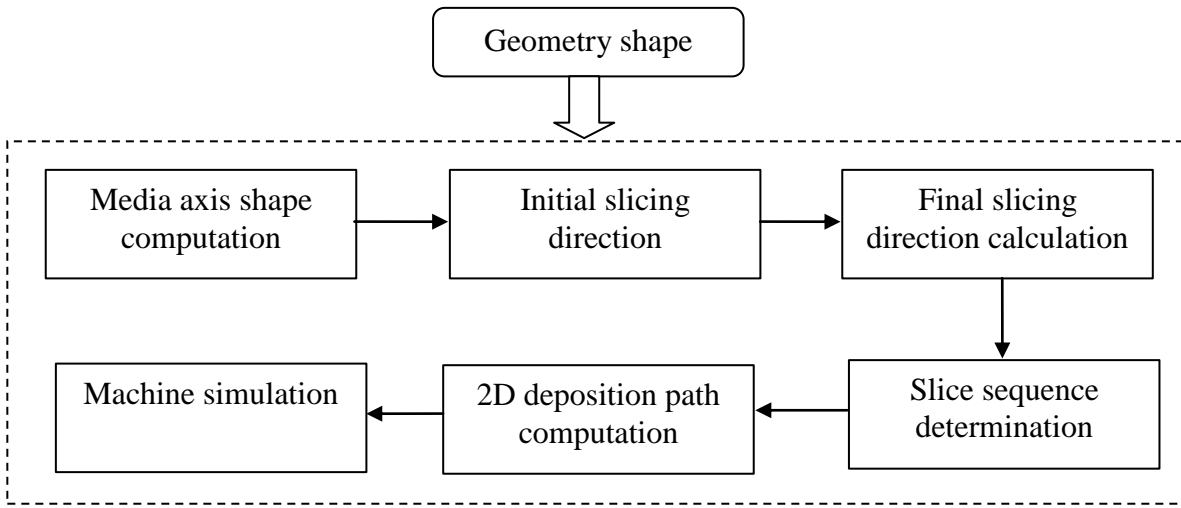


Figure 3: MAPS overall approach

III. Slicing Process

1. Centroidal axis computation

Since medial axis brings sufficient information (topological and geometrical), it is prudent to use medial axis for process planning in order to find optimal results. However, finding medial axis is

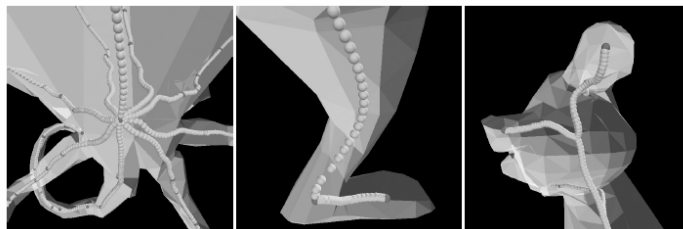


Figure 4: Skeleton of a bunny.

very computationally expensive. To compute skeletons of geometry shown in Figure 4, more than 200 seconds (in 2000 PC Windows environment) are needed. A more efficient geometry information extraction method is urgently needed in order to lead to an intelligent multi-axis slicing method. In MAPS, a concept of “centroidal axis” is researched.

Similar to medial axis, centroidal axis is also composed of a series of points which are centroids of cross sections at different locations. A cross section is the intersection of a planar surface with the object. A planar surface can be defined by a position and a normal direction. At a particular position, there are infinite directions; therefore, there are infinite cross sections, which may yield infinite centroidal axes for the object. To simplify the situation, the cross sections to define centroids are limited to these cross sections along three coordinate axes – X, Y, Z. Then, the centroidal axis is an aggregation of nodes which is composed of a geometric position and links connecting the node to other nodes. It can be expressed as

$$A = \{P_1, E_{11} \dots E_{1k} \mid \dots \mid P_i, E_{i1} \dots E_{ik} \mid \dots \mid P_n, E_{n1} \dots E_{nk}\} \quad i = 1 \dots n \quad E_{ii} = \langle P_i, P_i \rangle \quad i \neq l \quad (1)$$

where P_i is the centroid of a cross section and E_{il} is the link connecting P_i and P_l .

The computation of the centroidal axis is a tracing process. Illustrated in Figure 4.5, assuming that the initial direction to obtain a cross section is Z+ direction (upward) (\vec{D}_1), the direction is kept the same until the cross section S_A . If the direction is kept the same for cross section S_{A+1} , a vector $\vec{C}_A C_{A+1}$ can be formed by two centers C_A of S_A and C_{A+1} of S_{A+1} . The angle between $\vec{C}_A C_{A+1}$ and \vec{D}_1 is too large (greater than 45°), as shown in Figure 4.5(b). This indicates that a “direction change” is needed. Checking all other possible direction candidates (+X, -X, +Y, -Y), the +Y direction has the minimum angle with vector $\vec{C}_A C_{A+1}$; therefore, the new searching direction after cross section S_A is +Y. The same situation occurs when the cross section S_{B+1} is checked and the searching direction is changed to +Z direction after cross section S_B . Using such a technique and tracing all possible changes between the cross sections can form the centroidal axis as shown in Figure 4.5(c).

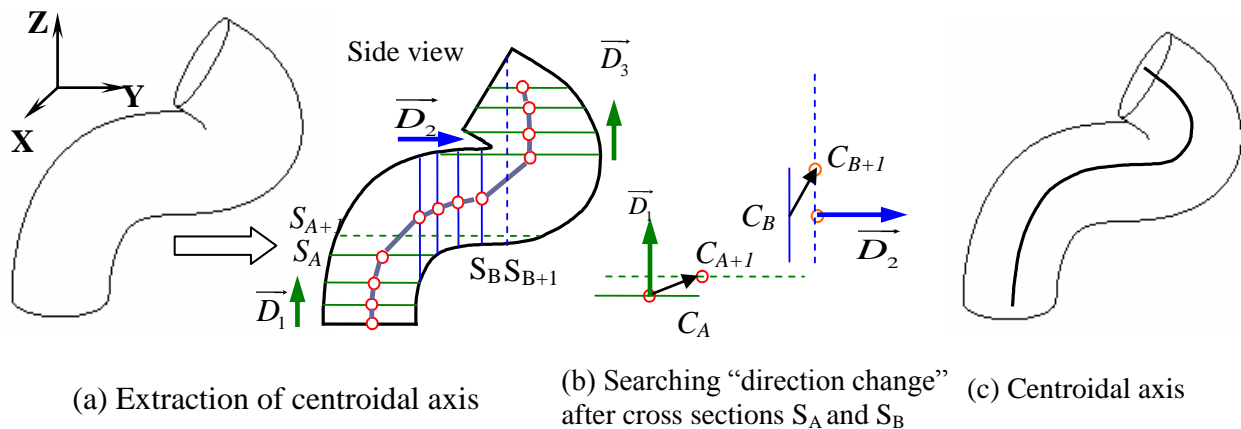


Figure 4: Computation of a centroidal axis

2. Slicing direction determination

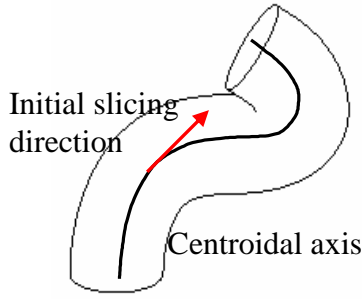


Figure 5: Initial slicing direction from a centroidal axis

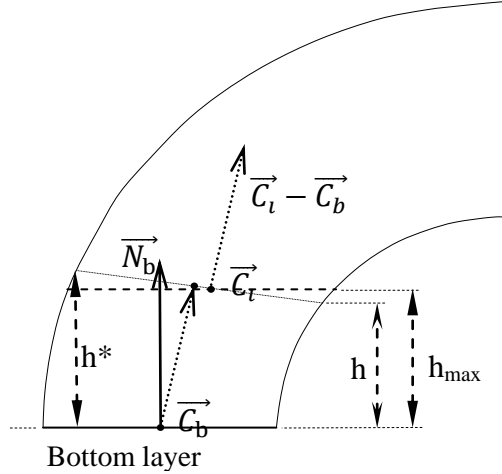


Figure 6: Final slicing direction searching

In MAPS, the initial slicing direction is obtained by mapping the slicing position to its associated centroidal axis, as shown in Figure 5 using the example shown in Figure 4. However, the final slicing direction and location are determined by error and layer thickness check.

Illustrated in Figure 6, the algorithm starts with the prediction step. Point \vec{G}_t is a guessed point for the next layer given by

$$\vec{G}_t = \vec{C}_b + h_{\max} * \vec{N}_b \quad (2)$$

The slicing direction is given by

$$\vec{D}_i = \vec{C}_t - \vec{C}_b \quad (3)$$

It is obvious that h^* is greater than h_{\max} , which is not acceptable for metal deposition process for a single layer slice. The layer height is shift down by

$$y = \left[\frac{h}{h^*} \right] y^* \quad (4)$$

where y is the next height, y^* is the current height.

The process is repeated until the h^* is less than h_{\max} and Ang_i is less than α .

3. Slicing sequence

In order to organize all slices, a hierarchy graph structure is constructed. In this structure, multiple parents and children relationship is implemented to represent the topological relationship among slices layers. Each node in the structure represents a slicing layer. The graph formed from top to bottom follows the slicing sequence and slicing direction change. Shown in Figure 7, the slice A is the parent of slice C; slice C and slice D are both parents of slice E. Different from a tree structure, a child can has multiple parents. In a regular graph structure, the links between nodes are bi-directional. However, the parent-children relationship is uni-directional in the hierarchy graph structures, which brings the following advantages:

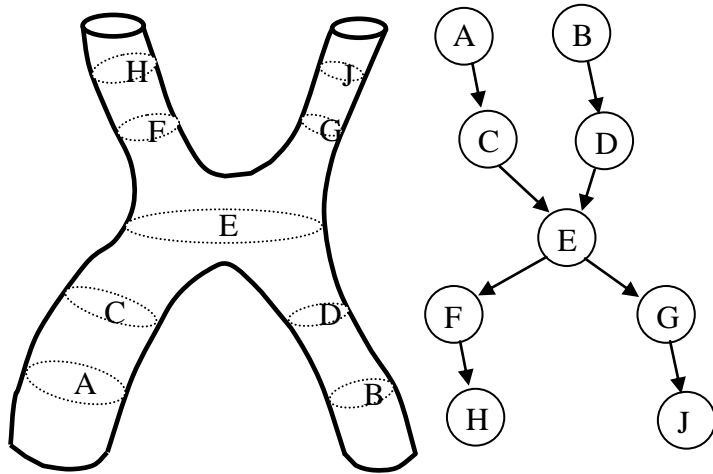


Figure 7: Hierarchy graph structure

- The slicing sequence among layers is clearly defined
- The hierarchy structure reduces the amount of the collision check, which is discussed later.
- The key slices (usually with multiple parents or children) in the hierarchy structure can be used to check the deposition quality

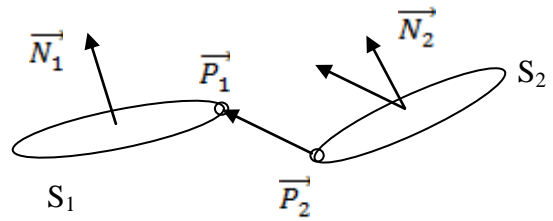


Figure 8: The collision check illustration

During the entire process, the deposition nozzle should not collide with the deposited portion of a part. Usually, the cladding nozzle of a typical laser metal deposition process is coaxial or close to such a shape. The powder fed using this type of nozzles forms a stream which is in the shape of a cone shape. Since the deposition process uses slices to represent the geometry, such a constraint can be translated as when depositing a slice, no collision should occur between the nozzle and other slices. It should be noted that the deposition process is a material additive process and the geometry is “continuously growing” until the fabrication is finished; thus, the child layer does not collide with its parent layer. The collision check problem between geometry becomes the collision check between slicing layers. In other words, the deposition of a slice should not collide with the deposition of other un-deposited slices.

As discussed above, the nozzle assembly can be simplified to a cone shape which is determined by a cone angle. Let S_1 be the slice to be deposited and S_2 is one of un-deposited slices, and \vec{N}_1, \vec{N}_2 are their slicing directions (normal) respectively. Then if one of conditions is met, the slice S_1 can be deposited without preventing the deposition of slice S_2 :

1. If S_2 is a child of S_1 or one of S_1 's leaves, then S_1 can be deposited.
2. Since a slice is a plane, it separates the space into two half spaces. Let the top half space be the one above a slice and the bottom space is the other half space below the slice. If the entire S_2 is in the top half space of S_1 , then S_1 can be deposited.
3. If the projection of S_1 along $-\vec{N}_2$ does not overlap with S_2 , find a pair of points on S_2 and S_1 respectively (\vec{P}_2 on S_2 and \vec{P}_1 on S_1). If angle between $\vec{P}_2\vec{P}_1$ and \vec{N}_2 is greater than $\theta/2$, then S_1 can be deposited, illustrated in Figure 8.

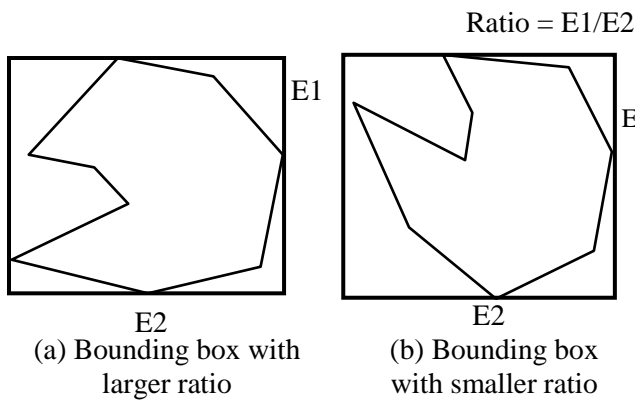


Figure 9: Bounding box with different ratio

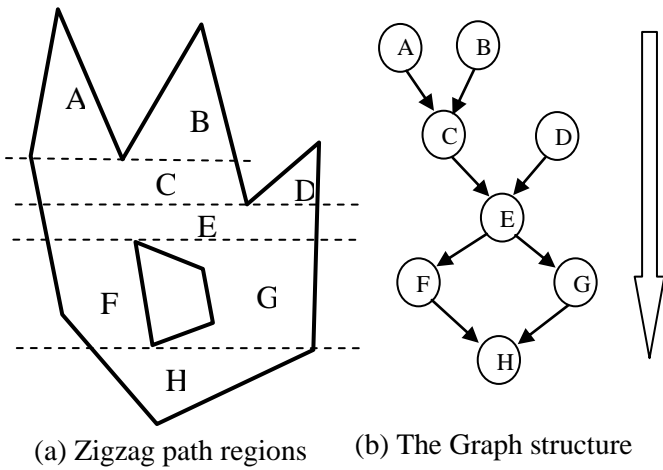


Figure 10: Hierarchy graph structure

4. 2D path planning

The two different 2D path patterns are adopted in MAPS. They are offset and zigzag. Each of them can be employed based on the shape of a slice. A typical zigzag path consists of a number of parallel segments. The path travel direction and connection determines the efficiency. Path orientation determines the entire path length. In laser deposition process, the “idle” or non-working path should be as short as possible due to the energy consumption and potential material waste. Path connection determines the length of “idle” paths; thus, the tool-path orientation and path connection are two critical techniques in generating zigzag path.

It can be observed that the tool-path with an inclination of 90° is having more number of non-depositing track paths compared to the one with 0° inclination. Also the total length of 90° is longer than the path of 0° inclination. In this research, the bounding box concept is used to select the inclination direction for zigzag path instead of using the longest edge of a 2-D shape. The ratio of the longer edge to shorter edge of the bounding box is different, as shown in Figure 9 and it is used to determine the inclination direction. In this research, the bounding box with the largest ratio is used to generate zigzag path. In order to find the bounding box with the largest ratio for a 2-D shape, the shape is rotated and the bounding box at each orientation is obtained. Once the zigzag path orientation is determined, a series of parallel paths can be generated. Connecting these paths has many different ways which results in the difference in efficiency. A hierarchy graph is designed for zigzag paths and is used as guide for path connection, illustrated in Figure 10.

The offset tool-path for machining processes has been researched widely. Simple offset or contour tool-path has been common practice in industry for a while. Although such path pattern has been used to generate tool-path for metal deposition process, the character of material additive process is still not fully incorporated into tool-path generation. The overlap of the tool-path in the machining process is to guarantee that the machining tool covers the entire area to be machined. In laser metal deposition process, the overlap also serves another purpose. The cross section of a deposition track for most metal materials is also bell-like; thus the overlap between tracks also helps to maintain the height. In MAPS, an initial offset path is revised to adjust the transverse speed in order to maintain a relatively even deposition height. The focus of adjust the

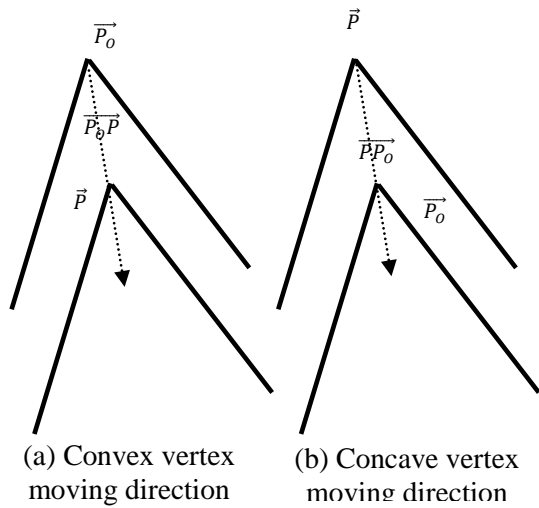


Figure 11: Toolpath adjustment

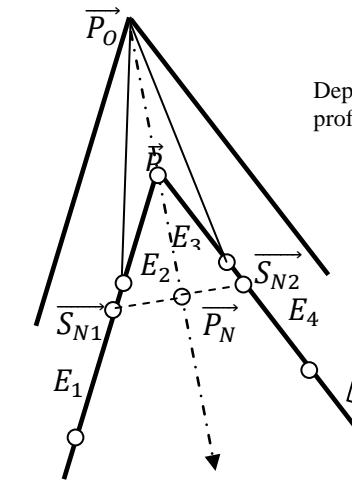


Figure 12: New points identification

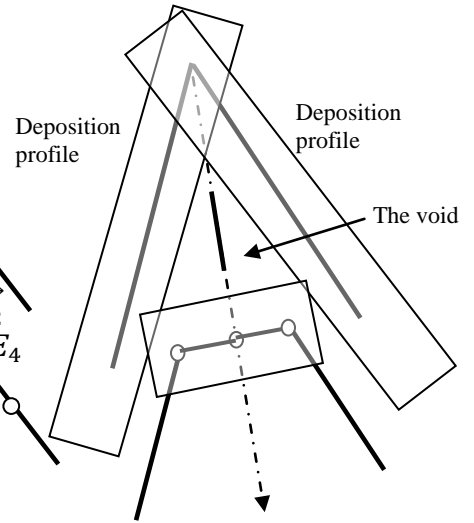


Figure 13: The void fill

offset toopath is to remove the vertices with a sharp angle since the machine speed will be slowed down at these locations.

Assuming a B-Spline or a polygon model in the the input geometry, the sharp angle point can be identified by tracing the angle between the edges. In this offset adjustment process, the tool-path along the boundary is not changed in order to maintain the required shape; thus the adjustment takes place on the path next to the boundary. Let \vec{P} be the point at a sharp angle on the offset path and \vec{P}_0 is the corresponding point on the outer path, shown in Figure 11. In order to adjust the tool-path and remove the sharp angle, it is obvious that the point \vec{P} should move along the direction $\vec{P}_0\vec{P}$ shown in Figure 11(b). However, the moving direction is $\vec{P}\vec{P}_0$ for the concave vertex. $\vec{P}_0\vec{P}$ or $\vec{P}\vec{P}_0$ is along with bisector line. Moving \vec{P} along this direction can have the equal impact on the neighboring path since the points on the bisector line have equal distance to both edges which form the angle. The first guessing point is given by

$$\vec{P}_N = \vec{P} + \vec{L} * a * T \quad (5)$$

where T is the track width, a is a coefficient for track width and $0.25 < a < 0.5$. a is determined by the sharpness of the angle. The sharper the angle, the greater a is.

When a new point \vec{P}_N is created, the edges which are around the vertex \vec{P} are checked. The following procedures for convex vertex are applied:

1. Find the vertices of the edge.
2. Identify points along the edges of the angle so that the length of vectors which they form with \vec{P}_0 are just longer than $\vec{P}_0\vec{P}$. In Figure 12, \vec{S}_{N1} , \vec{S}_{N2} are created points.
3. Form the new edges $\vec{S}_{N1}\vec{P}$, $\vec{S}_{N2}\vec{P}$ and put them into edges list and remove the un-needed edges, edge E_2 , E_3 are removed.

The other issue is that some void appears when the tool-path adjustment is performed. As shown in Figure 13, the void occurs in the center area. An extra path is created to fill the gap which is given by:

$$\vec{S} = \vec{P} + \vec{L} * \left(\frac{b}{\sin(\alpha/2)} + 1 \right) * T \quad (6)$$

$$\vec{E} = \vec{P}_N - \vec{L} * T \quad (7)$$

where \vec{S} and \vec{E} are the vertices of the edge, α is the angle at the corresponding point at the outer path. b is a coefficient for overlap effect.

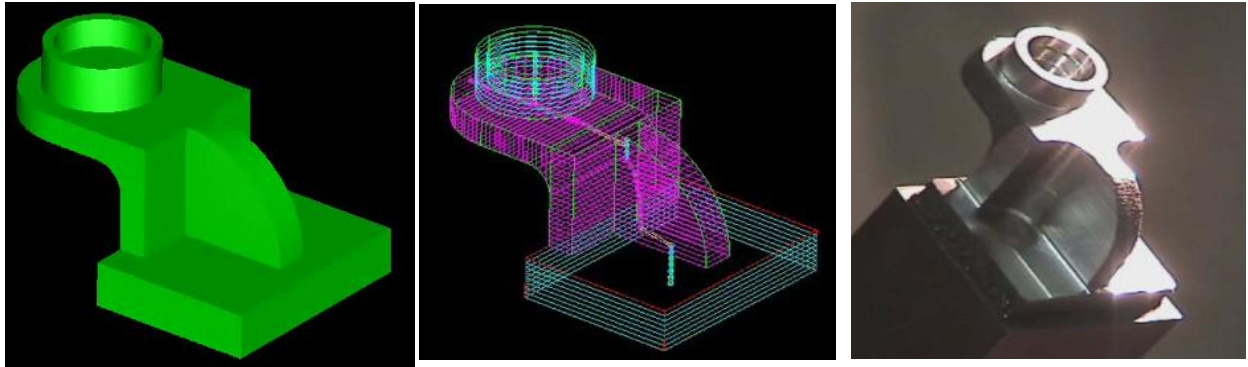
IV. Machine Simulation

To prevent wasted materials and time, or even machine damage, a simulation is critical to validate the process planning before executing code. In order to make the machine simulation module easily adapt to different machine configurations, the simulation has a generic representation for linear and rotational joints. Each specific machine is defined in a configuration file as a collection of these two types of joints. This configuration file tells the simulation software how to assemble the machine from its constituent components, how the parts move relative to each other, and what the names of the various axes are (eg. X, Y, Z, etc).

V. Examples

1. Slicing and deposition example

The presented algorithm has been implemented in VC++ using OpenCascade geometry kernel. Figure 14 shows the slicing result of a bearing seat example. It demonstrates the split surface construction. The slicing direction is changed correspondingly. All slicing directions are shown in the Figure. First, the slicing direction is Z up (from the bottom to the top) and then a slicing direction change is identified. The direction is rotated 90° in order to build the overhang. The last portion of the part is constructed along Z up direction again. Figure 15 shows an arch example with collision check. Figure 15 (b)-(e) shows the different sections in the sequence. In building process, the slicing algorithm puts the section 1 as the first section to be fabricated and the rest sections follow the sequence as shown in Figure 15. This example demonstrates the slicing direction slight change adjustment and the usage of hierarchy graph structure.

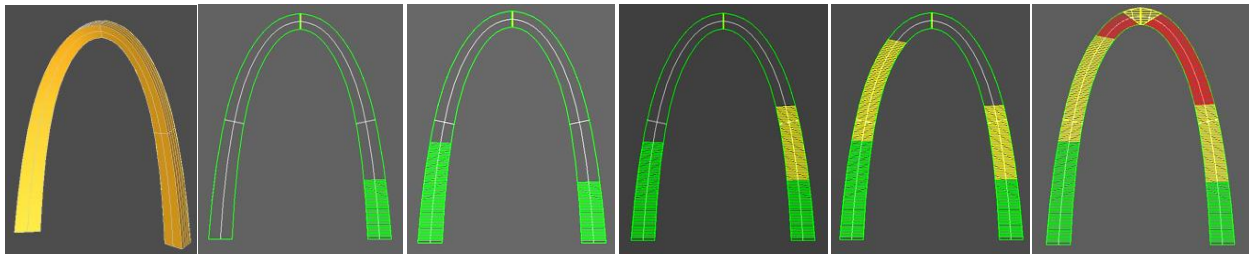


(a) Bearing seat CAD model

(b) Slicing result

(c) Fabricated part

Figure 14: Bearing seat example



(a) Solid model

(b) First section

(c) First and second section

(d) First 3 sections

(e) First 4 sections

(f) All slices

Figure 15: Arch example

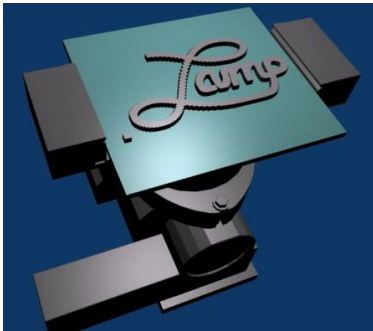


Figure 16: LAMP rotary table simulation

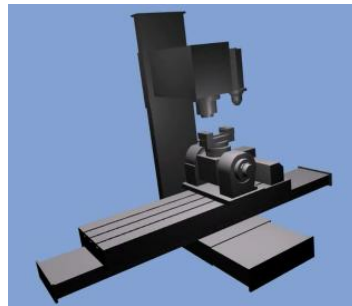


Figure 17: LAMP machine simulation

2. Machine simulation

In Figure 16, a rotation table with a vise setup is shown. The machine configuration is from Laser Aide Manufacturing Process (LAMP) at Missouri University of Science and Technology. Figure 17 shows the simulation result of LAMP CNC machine using the same machine simulator without redeveloping a post processor.

Conclusion

The multi-axis deposition system can potentially make solid freeform fabrication very attractive to industry. This paper presents the slicing of CAD models based on analysis of topological information between neighboring layers for such machines. The method presented in this paper provides the following characteristics:

1. The slicing direction change can be identified by checking the topological information.
2. An optimal building sequence can be determined using collision check.
3. The overhang structure can be fabricated by rotating the slicing direction.

By using topological information between neighboring layers, the multi-axis slicing process integrates the concepts of the “3-D” layer or decomposition of an object to make the slicing result accurate. The entire process is automatically driven by local geometry information without human interference. The algorithm is implemented on a geometry kernel, therefore it is very easy to extend its application on any geometry format including STL.

A machine simulator is developed to validate the process planning result and report the collision. The commonly seen post-processor is eliminated from this simulator by adopting a generic machine configuration description format. It has been proven the effectiveness by simulating two different hardware configurations.

Acknowledgement

This research was supported by the National Science Foundation grants DMI-9871185 and IIP-0637796, and a grant from the U.S. Air Force Research Laboratory contract # FA8650-04-C-5704. Support from Boeing Phantom Works, Product Innovation and Engineering, LLC, Spartan Light Metal Products Inc, MISSOURI S&T Intelligent Systems Center, and the MISSOURI S&T Manufacturing Engineering Program, is also greatly appreciated.

References:

- [1] Das, Suman; Harlan, Nicole; Beaman, Joseph and David Bourell, "Selective Laser Sintering of High Performance High Temperature Metals", *Proceedings of Solid Freeform Fabrication*, Austin, TX, 1996, pp 89-96.
- [2] Fodran, Eric; Koch, Martin and Menon, Unny, "Mechanical and Dimensional Characteristics of Fused Deposition Modeling Build Styles", *Solid Freeform Fabrication Proceedings*, 1996, pp 419-442.
- [3] Jacobs, P. F., "Stereolithography and Other RP&M Technologies: From Rapid Prototyping to Rapid Tooling" *Society of Manufacturing Engineers*, 1995.
- [4] McAlea, Kevin and Hejmadi, Uday, "Selective Laser Sintering of Metal Molds: The RapidTool (TM) Process", *Solid Freeform Fabrication Proceedings*, 1996, pp 97-104.
- [5] Pope, Matthew J.; Patterson, Mark C.L. Patterson; Zimbeck, Walter and Fehrenbacher, Mark, "Laminated Object Manufacturing of Si₃N₄ with Enhanced Properties", *Solid Freeform Fabrication Proceedings*, 1997, p 529-536.
- [6] Hofmeister, W., M. Griffith, M. Ensz, J. Smugeresky, Solidification in Direct Metal Deposition by LENS Processing, *JOM-Journal Of The Minerals Metals & Materials Society*, v. 53(#9) pp. 30-34 Sep 2001.
- [7] Laeng, J.; Stewart, J.G.; and Liou, F.W., "Laser Metal Forming Processes And The Application In Rapid Prototyping of Metallic Parts", *Proceedings of the 2nd International Conference on Advanced Manufacturing Technology*, Johor Bahru, Malaysia, August 2000a.
- [8] Laeng, J.; Stewart J.G.; and Liou, F.W., "Laser Metal Forming Processes for Rapid Prototyping – A Review," *International Journal of Production Research*, Vol.38, No.16, pp.3973, 2000b.
- [9] Pandey, Pulak Mohan; Reddy, N. Venkata and Dhande, Sanjay G., "Slicing procedures in layered manufacturing: a review", *Rapid Prototyping Journal*, Vol. 9 No. 5 2003, pp.274-288.
- [10] Dolenc, A and Mäkelä, I, "Slicing procedures for layered manufacturing techniques", *CAD*, Vol. 26, Feb. 1994, pp.119-126.
- [11] Kulkarni, Prashant and Dutta, Debasish, "An accurate slicing procedure for layered manufacturing", *CAD*, Vol.28, No.9, 1999, pp.683-397.
- [12] Kumar, Madhup and Choudhury, A. Roy, "Adaptive slicing with cubic path approximation", *Rapid Prototyping*, Vol. 8. No. 4, 2002, pp.224-232.
- [13] Ma, Weiyin and He, Peiren, "An adaptive slicing and selective hatching strategy for layered manufacturing", *Journal of Material Processing Technology*, 1999, pp.191-197.
- [14] Tata, Kamesh; Fadel, Georges; Bagchi, Amit and Aziz, Nadim, "Efficient slicing for layered manufacturing", *Rapid Prototyping*, Vol. 4. No. 4, 1998, pp.151-167.
- [15] Luo, Ren C.; Chang, Yi Cheng and Tzou, Jyh Hwa, "The development of a new adaptive slicing algorithm for layered manufacturing system", *Proceedings of the 2001 IEEE International Conference on Robotics & Automation*, Seoul, Korea, May 21-26, 2001.
- [16] Yang, Y.; Fuh, J.Y.H.; Loh, H. T. and Wong, Y. S., "A volumetric difference-based adaptive slicing and deposition method for layered manufacturing", *Journal of Manufacturing and Science*, Vol.125, Aug. 2003, pp.586-594.
- [17] Singh, Prabhjot; Dutta, Debasish, "Multi-Direction Slicing for Layered Manufacturing", *Journal of Computing and Information Science in Engineering*, June, 2001, Vol. 1, pp.129-142.

- [18] Zhang, J.; Ruan, J.; and Liou, F.W. "Process Planning for a Five-Axis Hybrid Rapid Manufacturing Process", *Proceedings of the Eleventh Annual Solid Freeform Fabrication Symposium*, Austin, TX, pp. 243., August 2000.
- [19] Zhang, Jun and Liou, F.W. "Adaptive Slicing for a Five-Axis Laser Aided Manufacturing Process," *Proceedings of the 2001 ASME Design Automation Conference*, Pittsburgh, Pennsylvania, September 9-12, 2001.
- [20] O'Rourke, Joseph, "*Computational geometry in C*", 2nd Ed., Cambridge Press, 1998.
- [21] Ma, Wan-Chn; Wu, Fu-Che and Ouhyoung Ming, "Skeleton extraction of 3D objects with radial basis function", *Proceedings of the Shape Modeling International 2003*.